EFFECTS OF THE SUPPORTS WITH DIFFERENT DIMENSIONS ON ELECTROCHEMICAL PERFORMANCE OF PLATINUM NANOPARTICLES

Yu-Chun Chiang[1, 2*], Pai-Hsuan Wu[1] and Heng-I Yueh[1]

[1]Department of Mechanical Engineering, Yuan Ze University, 135, Chung-Li, Taoyuan 320, Taiwan
Email: ycchiang@saturn.yzu.edu.tw,
[2]Fuel Cell Center, Yuan Ze University, 135, Chung-Li, Taoyuan 320, Taiwan
Email: ycchiang@saturn.yzu.edu.tw
* Corresponding author (ycchiang@saturn.yzu.edu.tw)

Keywords: Catalyst, Carbon nanotubes, Graphene, Characterization, Electrochemical activity

Abstract
In this study, the platinum (Pt) nanoparticles were deposited on oxidized carbon nanotubes (cCNT) or graphene sheets (cG) using the reverse micelle process. Results showed that the Pt nanoparticles on Pt/cCNT and Pt/cG were uniformly dispersed on the surface of the carbon materials, with mean sizes of Pt nanoparticles were 2.21 ± 0.92 and 2.08 ± 0.52 nm, respectively, where the mean size of Pt particles on Pt/C (JM) was 1.96 ± 0.50 nm. The crystallinity of Pt particles and the oxygen resistance of the samples followed the order of Pt/cG ~ Pt/cCNT > Pt/C. The metal Pt was the predominant Pt chemical state on all samples, where 52 at. % on Pt/cCNT、60 at. % on Pt/cG and 53 at. % on Pt/C (JM) were observed. The results from the cyclic voltammetry analysis showed that the values of electrochemical surface area (ECSA) were 88 m^2/g (Pt/cG) and 55 m^2/g (Pt/cCNT), much higher than that of Pt/C (JM, 46 m^2/g). The long-term test illustrated the degradation in ECSA exhibited the order of Pt/C (33 %) > Pt/cCNT (8 %) > Pt/cG (7 %).

1. Introduction

Proton exchange membrane fuel cells (PEMFCs) are an alternative power source for several applications because of their high energy-conversion efficiency and low pollution. The major challenges for the mass production and large-scale commercialization of PEMFCs are the high costs of the component materials and the poor performance. The performance of PEMFCs mainly relies upon the activity, utilization and durability of the electrocatalysts. Platinum (Pt) nanoparticles supported on carbon black (Pt/C) are the most commonly used electrocatalyst for PEMFCs. However, the global scarcity of Pt and its high cost demand for an urgent need to reduce the use of Pt and to improve the utilization of Pt. Electrochemical activity and stability of the catalysts applied on PEMFCs is one of the most important know-how for PEMFCs towards commercialization. In general, the enhancement of the activity can be achieved by reducing the particle sizes of the catalysts or improving the dispersion of the particles on the supports.

Several techniques have been used to prepare the Pt-based catalysts, including the wet-chemical processes, such as impregnation [1], the microwaveassisted polyol method [2], ion-exchange [3], ultrasonication/sonochemical route [4] and the colloidal method [5], as well as by the physical deposition processes, such as sputter deposition [6] and atomic layer deposition [7]. Most of these methods have been commonly used to prepare the Pt nanoparticles, but there is a wide range of particle sizes because the control of the growth of nuclei is inefficient. However, the colloidal processes (or called reverse micelle methods) are availably used to produce uniform Pt particles. Using

Excerpt from ISBN 978-3-00-053387-7

the colloidal method, Lin et al. [5] observed that Pt particles of 1-3 nm are homogeneously dispersed on the surface of carbon nanotubes (CNTs) that are treated with citric acid. The electrochemical surface area (ECSA) was 64 m^2/g, which remained unchanged after the durability test (0.4 V, 80 °C, 100 h), and the single cell of PEMFCs exhibited a high peak power density.

Li et al. [8] prepared composite graphene nanosheets decorated with Pt nanoparticles. Pt nano clusters, consisted of small Pt nanoparticles with mean diameters of about 5-6 nm, were deposited on the basal planes and the edges of the graphene. The value of the ECSA for the Pt/graphene was 44.6 m^2/g, higher than that of commercial Pt/C (30.1 m^2/g). Kou et al. [9] studied the electrochemical activity of Pt nanoparticles supported on functionalized graphene sheets (FGS) by impregnation methods. The improved performance of Pt/FGS compared to Pt/C (E–TEK) can be attributed to the smaller particle size (average Pt size ~ 2 nm) and less aggregation of the Pt nanoparticles on FGS. It was also observed Pt-Ru/graphene nanosheets exhibited higher ECSA (47.9 m^2/g, 1.7 times that of Pt-Ru/Vulcan) and methanol oxidation activity (0.113 mA g/m^2, 1.4 times that of Pt-Ru/Vulcan) [10]. Seo et al. [11] found the values of ECSA for Pd/graphene was 54.9 m^2/g, higher than that of Pt/graphene (42.0 m^2/g). In addition, some studies also investigated the effects of the spacers between metal nanoparticles and the graphene sheets, such as carbon nanotubes [12], carbon black [13], or indium tin oxide (ITO) [14].

In this study, the CNTs and graphene sheets were applied to overcome the corrosion problems of carbon black at operating conditions of PEMFCs. To enhance the interfacial interactions between the CNTs or graphene sheets and the Pt nanoparticles, the oxygen-containing functional groups were introduced onto the surface of graphene sheets. Therefore, the citric acid-treated carbon nanotubes (cCNT) and graphene sheets (cG) were prepared and then the Pt nanoparticles were deposited on cCNT and cG by a colloidal method. One commercial Pt/C catalyst (Johnson Matthey, JM) was used for comparison. The products were characterized by high-resolution transmission electron microscopy (HRTEM), thermogravimetric analysis (TGA), X-ray Diffraction (XRD) and X-ray photoelectron spectroscopy (XPS). The cyclic voltammetry (CV) technique was used to measure the ECSA and stability of the catalysts. Moreover, the Pt utilization efficiency was discussed.

2. Experimental

2.1. Oxidation of Carbon Supports

The commercial multi-walled CNTs and graphene sheets chosen as the carbon supports in this study were provided by Legend Star International Co. The oxygen-containing functional groups were introduced onto the surface of the carbon supports by treating with citric acid ($C_6H_8O_7$), as follows: 200 mg of the carbon support was added to 3 ml of the citric acid aqueous solution (1.6 mM) and subjected to 15 min ultrasonic treatment, followed by vigorous stirring for 1 h using a magnetic stirrer. The ultrasonic treatment was conducted using a bath type sonicator (BRANSON 5510) at a frequency of 46 kHz and a power of 150 W. And then the samples were heat-treated in a muffle furnace at 300 ^oC for 30 min. The oxidized MWCNTs and graphene sheets were denoted as cCNT and cG.

2.2. Decoration of Pt nanoparticles on functionalized CNTs

The deposition of Pt nanoparticles onto the surface of cCNT or cG (20 wt. %) was performed using the colloidal method [5], which involves a two-phase transfer of $PtCl_6^{2-}$, followed by reduction in the presence of 1-dodecanethiol (DDT, $C_{12}H_{25}SH$, 98 %). Hexachloroplatinic acid ($H_2PtCl_6 \cdot 6H_2O$) solution (3 ml of 0.086 M in deionized water) was mixed with tetraoctylammonium bromide (ToAB, $N(C_8H_{17})_4Br$) solution (4 ml of 0.18 M in toluene) and vigorously stirred for about 30 min at room temperature. During this process, $PtCl_6^{2-}$ ions are transferred from aqueous solution to the organic layer (toluene), using ToAB as the phase-transfer catalyst. The orange-colored organic layer was extracted and 450 mg of DDT (capping agent) was added and stirred for 30 min. 200 mg cCNT or cG

Excerpt from ISBN 978-3-00-053387-7

was then added with constant stirring for 1 h. 10 ml of 0.25 M sodium formate (HCOONa) aqueous solution was added drop-wise at 60 °C, to reduce the Pt ion. The solid product was filtered and rinsed with ethanol to remove excess of DDT and with copious amount of warm deionized water to remove the remaining sodium formate. The black solid products were vacuum dried at 100 °C for 3 h and further heat-treated at 800 °C for 2 h in a tubular furnace in an argon atmosphere. One commercial Pt/C (Johnson Matthey, denoted as JM) with a Pt content of 20 wt. % was used for comparison.

2.3. Material Characterizations

HRTEM images were obtained using a transmission electron microscope (Hitachi H-7100, 200 kV), to determine the interior microstructure of the carbon supports and the morphology and size distribution of the Pt nanoparticles deposited on them. The oxidation resistance of the samples was determined in flowing air (60 cm^3/min) with a heating rate of 10 °C/min, using a thermogravimetric analyzer (Dynamic TGA Q500 in TA Instrument 5100) to measure any changes in the weight of the sample as a function of temperature (TGA plot) and the rate of weight loss versus temperature (differential thermogravimetry, DTG, plot). The residual mass was used to estimate the Pt content deposited on the surface of cCNT or cG. The XRD patterns were taken with an X-ray powder diffractometer (Rigaku (Japan) TTRAX III) to give detailed information about the crystallographic structure of the materials. The radiation used was Cu Kα with a wavelength of 0.15418 nm, a voltage of 30 kV and a current of 20 mA. The value of 2-theta (2θ) ranges from 10° to 90°, where θ is the diffraction angle, with a scanning speed of 4°/min. XPS was used to determine the number and type of functional groups present on the surface of the samples, using a PHI 5000 VersaProbe (ULVAC-PHI) instrument, equipped with Al Kα (1486.6 eV) monochromator, Anode (25W, 15kV), operating at background pressure is $6.7x10^{-8}$ Pa. For calibration purposes, the C 1s electron binding energy that corresponds to graphitic carbon was set at 284.6 eV. A nonlinear least squares curve-fitting program (XPSPEAK software, Version 4.1) was used for deconvolution of the XPS spectra.

2.4. Measurement of Electrochemical Activity

A CHI 613C electrochemical workstation (CH Instruments) was employed for the electrochemical study of carbon supported Pt samples. A three-electrode electrochemical cell was constructed for CV measurements, through which the ECSA of the Pt nanoparticles was determined. The working electrode was a thin layer of Nafion®-impregnated catalyst sample, cast on a vitreous carbon disk of 5 mm in diameter embedded in a Teflon cylinder. A homogeneous ink composed of electrocatalyst, Nafion® ionomer (5 wt. %, DuPont), and isopropanol, where the Nafion® content in the thin-film electrocatalyst layer was 25 wt. %. A Pt wire and a saturated calomel electrode (SCE) were used as the counter and reference electrodes, respectively. The measurements of CV were conducted at room temperature using 0.5 M H_2SO_4 as the electrolyte solution at a scan rate of 20 mV/s from -0.2-1.0 V vs. SCE.

3. Eesults and Discussion

The HRTEM images of the samples were shown in Figure 1. Well-dispersed Pt nanoparticles were uniformly distributed on the walls of the carbon supports. The mean sizes of the Pt particles were 2.21 ± 0.92 nm for Pt/cCNT and 2.08 ± 0.52 nm for Pt/cG. As seen from the data, the Pt nanoparticles deposited on oxidized graphene sheets had a slightly smaller mean particle size with a more centralized distribution compared to Pt/cCNT but both had a high degree of uniformity. It observed that the Pt nanoparticles on commercial Pt/C (JM) with a mean size of 1.96 ± 0.50 nm were smaller than those deposited on the carbon supports used in this study, and the distribution of the Pt particle sizes was similar to Pt/cG.

Excerpt from ISBN 978-3-00-053387-7

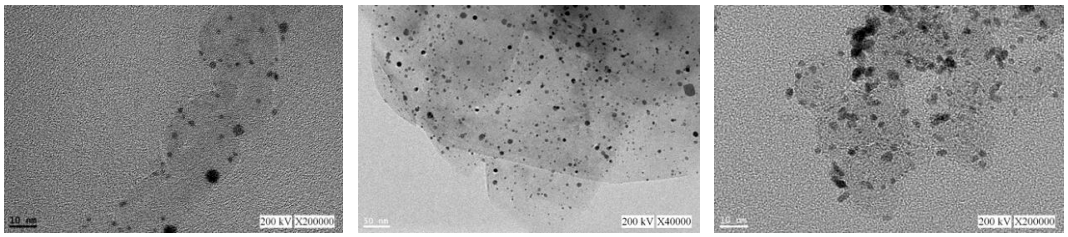

(a) Pt/cCNT (b) Pt/cG (c) Pt/C (JM)

Figure 1. HRTEM images of the samples.

The oxidation resistance of the samples could be evaluated by TGA data. The TGA and DTG profiles for all samples were measured in flowing air of 60 sccm and heated at a rate of 10 ◦C/min. The temperatures for the maximum rate of weight loss (or oxidation) for Pt/cCNT, Pt/cG and Pt/C (JM) were 595, 581 and 414 ◦C, which implied the thermal stabilities of Pt/cCNT and Pt/cG were better than that of Pt/C (JM) in air. In addition, the full width at half maximum of the DTG profiles followed the order Pt/cG > Pt/cCNT > Pt/C, indicative of the degree of resistance to oxidation again. The profiles for the TGA weight loss of Pt/cCNT and Pt/cG showed that the residue were 11.6 and 12.2 wt. %. These data, combined with the metal catalyst residue in each carbon support (not shown here), were used to calculate the Pt contents, which were 9.6 and 9.7 wt. %.

A high degree of crystallinity for the samples was shown in the XRD patterns. The diffraction peak at a 2θ value of ~ 26º was attributed to the graphite-like structure, C(002). All of the samples exhibited strong diffraction at 2θ values of 39.8º, 46.2º, 67.5º and 81.3º, which could be indexed as the reflections from the Pt(111), Pt(200), Pt(220) and Pt(311) planes. This indicates that the Pt catalysts have a face-centered cubic structure. The diffraction peaks for Pt/C (JM) were broader than those for Pt/cCNT and Pt/cG, which indicated that the average sizes of the Pt particles on cCNT and cG were greater than that on Pt/C (JM). In summary, the XRD results showed that the Pt precursor was reduced to the metallic state using the colloidal method.

The XPS survey scan spectra of the samples revealing the compositions of the most external surface showed the major peaks in the spectra were due to the C1s, O1s and Pt4f photoelectrons. The elemental compositions (atomic ratio, at. %) on the surface or over the sampling depth of several atomic layers from the surface were 97.3 (C): 2.0 (O): 0.7 (Pt) for Pt/cCNT, 93.5 (C): 5.5 (O): 1.0 (Pt) for Pt/cG, 91.2 (C): 5.9 (O): 2.9 (Pt) for Pt/C (JM). The oxidation of weak citric acid would be able to fix the Pt nanoparticles but not increase oxygen content significantly. In addition, the higher oxygen content in Pt/C (JM) were responsible for its less thermal stability. The deconvolution of the XPS spectra over the Pt4f region showed different states of oxidation for each of the carbon supported Pt samples, which consisted of three couples of doublets. The most intense doublet, at 71.0 and 74.35 eV, represents a zero-valence metallic Pt (Pt^o), the doublet at 72.4 and75.75 eV is attributed to the presence of an amorphous Pt (II) species, such as PtO or $Pt(OH)_2$ [15], and the broader doublet at 74.9 and 78.25 eV is assigned to the Pt (IV) species. The results showed that the distributions of Pt chemical states were similar for all samples. The predominant Pt state was in the zero-valence metallic state, in the order of 60.4 (Pt/cG) > 53.3 (Pt/cCNT) > 52.2 (Pt/C, JM) at. %. The atomic percentages of Pt (II) and Pt (IV) in all samples were close to each other, indicating the reduction degrees of Pt precursor on these three carbons with different dimensions were almost completely.

The cyclic voltammograms for all samples displayed three characteristic potential regions: the hydrogen adsorption/desorption region (-0.2 to 0.1 V), double layer plateau region (0.1 to 0.5 V) and the formation and reduction of surface Pt oxides (0.5 to 1.0 V). All voltammograms displayed a well-defined hydrogen adsorption/ desorption region from -0.2 to 0.1 V vs. SCE. Compared to that of the

Excerpt from ISBN 978-3-00-053387-7

Pt/cCNT and Pt/C, the Pt nanoparticles deposited on oxidized graphene sheets possessed a wider double layer region, which indicated a higher ability of a system to store electric charges. The ECSA is a very significant parameter which reflects the intrinsic electrocatalytic activity of a Pt catalyst. The ECSA for Pt/cCNT, Pt/cG and Pt/C were calculated to be 55, 88 and 46 m^2/g, respectively, based on a monolayer hydrogen adsorption charge of 0.21 mC/cm^2 on polycrystalline Pt. The experimental data indicated that the electrochemical activity of Pt nanoparticles deposited on cCNT or cG was higher than that on carbon black. A higher ECSA of the Pt/cG could be attributed to the 2D structure of graphene sheets provided much more active sites accessible to Pt ions and its excellent electric conductivity.

Long-term tests were conducted at the same conditions (at a scan rate of 20 mV/s from -0.2 ~ 1.0 V vs. SCE) in order to understand the electrochemical stability of carbon supported Pt nanoparticles. The dependence of ECSA on the number of cycles, shown in Table 1, displayed the degradation in ECSA due to dissolution/reprecipitation or migration of Pt particles or the diffusion of Pt ionic species [16]. The electrochemical stability of carbon supported Pt nanoparticles presented the order of Pt/cG > Pt/cCNT > Pt/C (JM). In addition, the Pt utilization efficiency (η) is also the essential parameter to describe the electrocatalytical performance and calculated by dividing ECSA by the chemical surface area (CSA) [17]. The CSA is defined as $6/\rho d$, where ρ is the density of Pt (= 21.09 g/cm^3) and d is mean diameter of Pt nanoparticle (nm). Thus, the values of the η were 38.9 % for Pt/cCNT, 64.3 % for Pt/cG and 31.7 % for Pt/C. The results implied the citric acid-treated graphene sheets was an effective support for Pt depositions.

Table 1. Calculated ECSA (m^2/g) and activity degradation (%) of the samples.

Sample	Parameter	30th	100th	200th	300th	400th	500th	600th
Pt/cCNT	ECSA (m^2/g)	48	55	52	53	52	52	51
	Degradation (%)	—	—	5	4	6	6	8
Pt/cG	ECSA (m^2/g)	82	88	87	85	84	84	82
	Degradation (%)	—	—	2	3	5	5	7
Pt/C (JM)	ECSA (m^2/g)	46	40	34	33	33	33	31
	Degradation (%)	—	13	26	28	29	28	33

4. Conclusions

Results showed that the Pt nanoparticles were uniformly dispersed on the surface of carbon supports, with the mean sizes of Pt particles were 2.21 ± 0.92 nm (Pt/cCNT), 2.08 ± 0.52 nm (Pt/cG) and 1.96 ± 0.50 nm (Pt/C, JM). The crystallinity and the degree of oxygen resistance of the Pt-based catalysts followed the order of Pt/cG > Pt/cCNT > Pt/C (JM). The contents of the metal Pt most predominant Pt chemical state on all samples were 52 (Pt/cCNT), 60 (Pt/cG) and 53 (Pt/C, JM) at. %. The results from CV analysis showed that the values of electrochemical surface area (ECSA) of Pt/cCNT, Pt/cG and Pt/c (JM) were 50, 88 and 46 m^2/g, respectively. The long-term test illustrated the degradation in ECSA exhibited the order of Pt/C (33 %) > Pt/cCNT (8 %) > Pt/cG (7 %). Moreover, the values of the Pt utilization efficiency were 38.9 % for Pt/cCNT, 64.3 % for Pt/cG and 31.7 % for Pt/C (JM). The high electrochemical activity and utilization of Pt deposited on 1D (CNTs) and 2 D (graphene sheets) carbon supports could be derived from the coordination of the Pt ions with the functionalities on the surface of carbon supports. Moreover, the performance of Pt/cG was superior to that of Pt/cCNT.

Excerpt from ISBN 978-3-00-053387-7

References

[1] H.Y. Du, C.H.Wang, H.C. Hsu, S.T. Chang, U.S. Chen, S.C. Yen, L.C. Chen, H.C. Shih, and K.H.Chen. Controlled platinum nanoparticles uniformly dispersed on nitrogen-doped carbon nanotubes for methanol oxidation. *Diamond & Related Materials*, 17:535–541, 2008.

[2] X. Li, W.X. Chen, J. Zhao, W. Xing, and Z.D. Xu. Microwave polyol synthesis of Pt/CNTs catalysts: effects of pH on particle size and electrocatalytic activity for methanol electrooxidation. *Carbon*, 43:2168-2174, 2005.

[3] R. Yu, L. Chen, Q. Liu, J. Lin, K.L. Tan, S.C. Ng, H.S.O. Chan, G.Q. Xu, and T.S.A. Hor. Platinum deposition on carbon nanotubes via chemical modification. *Chemistry of Materials*, 10:718-722, 1998.

[4] B.G. Pollet. The use of ultrasound for the fabrication of fuel cell materials. *International Journal of Hydrogen Energy*, 35:11986-12004, 2010.

[5] J.F. Lin, V. Kamavaram, and A.M. Kannan. Synthesis and characterization of carbon nanotubes supported platinum nanocatalyst for proton exchange membrane fuel cells. *Journal of Power Sources*, 195:466-470, 2010.

[6] K. Makino, K. Furukawa, K. Okajima, and M. Sudoh. Optimization of the sputterdeposited platinum cathode for a direct methanol fuel cell. *Electrochimica Acta*, 51:961–965, 2005.

[7] Y.C. Hsueh, C.C. Wang, C.C. Kei, Y.H. Lin, C. Liu, and T.P. Perng. Fabrication of catalyst by atomic layer deposition for high specific power density proton exchangemembrane fuel cells. *Journal of Catalysis*, 294:63–68, 2012.

[8] Y. Li, L. Tang, and J. Li. Preparation and electrochemical performance for methanol oxidation of Pt/graphene nanocomposites. *Electrochemistry Communications*, 11:846-849, 2009.

[9] R. Kou, Y. Shao, D. Wang, M.H. Engelhard, J.H. Kwak, J. Wang, V.V. Viswanathan, C. Wang, Y. Lin, Y. Wang, I.A. Aksay, and J. Liu. Enhanced activity and stability of Pt catalysts on functionalized graphene sheets for electrocatalytic oxygen reduction. *Electrochemistry Communications*, 11:954-957, 2009.

[10] S. Bong, Y.R. Kim, I. Kim, S. Woo, S. Uhm, J. Lee, and H. Kim. Graphene supported electrocatalysts for methanol oxidation. *Electrochemistry Communications*, 12:129-131, 2010.

[11] M.H. Seo, S.M. Choi, H.J. Kim, and W.B. Kim. The graphene-supported Pd and Pt catalysts for highly active oxygen reduction reaction in an alkaline condition. *Electrochemistry Communications*, 13:182-185, 2011.

[12] S.Y. Yang, K.H. Chang, Y.F. Lee, C.C.M. Ma, and C.C. Hu. Constructing a hierarchical graphene–carbon nanotube architecture for enhancing exposure of graphene and electrochemical activity of Pt nanoclusters. *Electrochemistry Communications*, 12:1206-1209, 2010.

[13] S. Park, Y. Shao, H. Wan, P.C. Rieke, V.V. Viswanathan, S.A. Towne, L.V. Saraf, J. Liu, Y. Lin, and Y. Wang. Design of graphene sheets-supported Pt catalyst layer in PEM fuel cells. *Electrochemistry Communications*, 13:258-261, 2011.

[14] R. Kou, Y. Shao, D. Mei, Z. Nie, D. Wang, C. Wang, V.V. Viswanathan, S. Park, I.A. Aksay, Y. Lin, Y. Wang, and J. Liu. Stabilization of electrocatalytic metal nanoparticles at metal-metal oxide-graphene triple junction points. *Journal of the American Chemical Society*, 133:2541-2547, 2011.

[15] Z. Liu, J.Y. Lee, W. Chen, M. Han, and L.M. Gan, Physical and electrochemical characterizations of microwave-assisted polyol preparation of carbon-supported PtRu nanoparticles. *Langmuir*, 20:181-187, 2004.

[16] O.J. Curnick, P.M. Mendes, and B.G. Pollet. Enhanced durability of a Pt/C electrocatalyst derived from Nafion-stabilized colloidal platinum nanoparticles. *Electrochemistry Communications*, 12:1017-1020, 2010.

[17] J.J. Wang, G.P. Yin, J. Zhang, Z.B. Wang, and Y.Z. Gao, High utilization platinum deposition on single-walled carbon nanotubes as catalysts for direct methanol fuel cell. *Electrochimica Acta*, 52:7042 – 7050, 2007.

Excerpt from ISBN 978-3-00-053387-7